Mon. Not. R. Astron. Soc. (1992) **259**, 233–246

# The cluster of galaxies SC2008 − 57 (A3667)★

Laerte Sodré, Jr,[1]† Hugo V. Capelato,[2] João E. Steiner,[3] Dominique Proust[4] and Alain Mazure[5]

[1] *Royal Greenwich Observatory, Madingley Road, Cambridge CB3 0EZ*
[2] *Departamento de Astrofísica INPE/MCT, CP151, 12201 São José dos Campos, Brazil*
[3] *Instituto Astronomico e Geofisico da USP, CP9638, 01065 São Paulo, Brazil*
[4] *Observatoire de Paris, Section de Meudon, DAEC, F92195 Meudon Cedex, France*
[5] *Laboratoire d'Astronomie, USTL, F34060 Montpellier Cedex, France*

Accepted 1992 May 8. Received 1992 April 30; in original form 1992 February 13

**ABSTRACT**

We present the results of photometric and spectroscopic observations of the cluster of galaxies SC2008 − 57 (A3667). The observations have resulted in a catalogue with positions and magnitudes for 203 galaxies, complete at $b_{25} = 18.0$, and radial velocities for 128 galaxies, 91 per cent complete at $b_{25} = 17.5$. The cluster can be classified as type L because its galaxy distribution is highly flattened. It shows two strong concentrations: a main concentration, centred on the cluster brightest galaxy (a D galaxy) and coincident with the peak of X-ray emission, and a substructure around the second brightest galaxy (also a D galaxy). Most of the galaxies in this substructure seem to be bound to the second-brightest galaxy, forming a dynamical subunit inside the cluster. The extreme flattening of the cluster may at least partially be due to the presence of the substructure. The cluster also shows evidence for luminosity segregation, with the brightest galaxies being preferentially found in high galaxy density regions. Most of the luminosity segregation, however, is produced by galaxies associated with the two clumps around the D galaxies, suggesting that dynamical friction is effective in subclusters with low velocity dispersions and may be associated with the formation of D galaxies. The velocity dispersion of SC2008 − 57 is high, about 1200 km $s^{-1}$, but consistent with the observed X-ray luminosity. The cluster mass, derived using several estimators, is about $2.6 \times 10^{15}$ $M_{\odot}$. Both the cluster mass and velocity dispersion may be overestimates due to the presence of the substructure.

**Key words:** catalogues – galaxies: clustering – galaxies: distances and redshifts – galaxies: luminosity function, mass function – galaxies: photometry.

## 1 INTRODUCTION

Clusters are the densest concentrations of galaxies usually found in the Universe. Knowledge of their structure and degree of clumpiness may provide pieces of information essential to our understanding of galaxy clustering, of the dynamical processes inside these structures and of the distribution of dark matter, and even clues on the origin of galaxies of distinct morphological types.

The galaxy cluster SC2008 − 57 (A3667 in the new catalogue of Abell, Corwin & Olowin 1989) is among the strongest extragalactic X-ray sources in the southern sky (Bahcall 1977; Mushotzky 1984). The first X-ray spectrum of this object was obtained in 1974 by the MSSL experiment aboard *Ariel V* in the 2–30 keV range (Bell-Burnell & Chiappetti 1984). The *HEAO1* observations are reviewed by Mushotzky (1984). In the range 2–10 keV the spectrum is well described by thermal bremsstrahlung emission of a gas with $kT = 6.2 \pm 0.7$ keV. The *HEAO1-A2* experiment also detected an iron line with an equivalent width of $500^{+170}_{-230}$ eV, corresponding to an iron abundance of $0.57^{+0.2}_{-0.27}$ times the solar value. The cluster was also observed with the ME detectors aboard the *EXOSAT* satellite (Piro & Fusco-Femiano 1988). The spectrum in the 1.2–10 keV range gives

★ Based on observations made at Cerro Tololo Inter-American Observatory (CTIO), National Optical Astronomy Observatories, which is operated by the Association of Universities for Research in Astronomy, Inc. (AURA).
† On leave of absence from Instituto Astronomico e Geofisico da USP (IAG), CP9638, 01065 São Paulo, Brazil.

a gas temperature of $kT = 5.3^{+1.1}_{-0.9}$ keV, consistent with the *HEAO1* observations. All these observations indicate a steady flux of $(7.4 \pm 0.5) \times 10^{-11}$ erg cm$^{-2}$ s$^{-1}$.

Several previous optical studies of SC2008 − 57 are reported in the literature. Bahcall (1977) estimated a cluster redshift of about 0.06 by comparing the magnitudes of the cluster brightest members with those of clusters at known redshifts on the ESO(B) plates. She also classified the cluster as type L (line) in the Rood–Sastry system (Rood & Sastry 1971), since its brightest galaxies are arranged in a line. Melnick & Quintana (1981) measured radial velocities for 23 galaxies in the cluster field, obtaining a redshift corrected for solar motion of 0.053 and a velocity dispersion of 1470 km s$^{-1}$. They noted that the cluster has two D-type galaxies separated by 16 arcmin and by 400 km s$^{-1}$ in radial velocity. Although the cluster as a whole appears to be centred on the brightest galaxy, they observed a local density enhancement around the second-brightest galaxy. They pointed out that their value for the cluster velocity dispersion is somewhat high to satisfy well the $L_X$–$\sigma$ relationship. Multi-aperture photoelectric observations of six galaxies in the cluster field were performed by Melnick & Quintana (1984). This cluster was also observed by Proust et al. (1988) with the OPTOPUS, resulting in 48 galaxies in the cluster field with known radial velocities.

In this paper we report new results of photometric and spectroscopic observations made at Cerro Tololo Inter-American Observatory (Section 2). These observations allowed us to construct a catalogue with 203 galaxies complete up to $b_{25} = 18.0$ and with 128 radial velocities. Our original motivation for measuring new velocities in SC2008 − 57 was to have a sample large enough to test for cluster rotation and/or peculiar motions (Sodré et al. 1990). Our velocity sample is 91 per cent complete at $b_{25} = 17.50$. In Section 3 we discuss the galaxy distribution, showing that there is a substructure around the cluster second-brightest galaxy. The luminosity distribution of the observed galaxies is discussed in Section 4, where we argue that the cluster is luminosity-segregated. Most of the luminosity segregation, however, seems to be produced by galaxies within the two clumps around the D galaxies. In Section 5 we analyse the velocity distribution, compute dynamical mass estimates and show that the substructure observed in the galaxy distribution has a kinematical counterpart. Finally, in Section 6 we summarize our conclusions. When needed, we have used $H_0 = 100$ km s$^{-1}$ Mpc$^{-1}$ and $q_0 = 0.5$ throughout this paper.

## 2 OBSERVATIONS AND REDUCTIONS

### 2.1 Photometric observations

A photographic plate centred on SC2008 − 57 was obtained by JES in 1983 September with the CTIO Curtis–Schmidt telescope (F3.5, plate scale = 96.6 arcsec mm$^{-1}$). One 60-min exposure was taken using a IIIaJ emulsion and a GG385 filter. The seeing was about 1.5 arcsec, as inferred from the width of non-saturated stellar images in the plate. Another plate, with the same emulsion/filter combination, was exposed to known intensities with the CTIO Weston sensitometer in order to provide the sensitometric spots for the density-to-intensity calibration. The combination IIIaJ + GG385 defines a photometric band which is often called $b_J$ since it is similar to the Johnson $B$ band.

This plate was digitized on the PDS microdensitometer of Observatorio Nacional (Rio de Janeiro) with a pixel size of 20 μm (1.932 arcsec). Although the plate covers a field of about 25 square degrees on the sky, only an area of about 1.8 square degrees ($5 \times 5$ cm$^2$) centred on the cluster brightest galaxy was digitized, resulting in a 10-bit image with $2500 \times 2500$ pixels. At the distance of SC2008 − 57 ($z = 0.055$) the digitized region corresponds to a square of 3.5 Mpc on a side, therefore enclosing the Abell radius area.

The density-to-intensity calibration was obtained by a least-square fitting of the sensitometric spot densities (measured by the PDS) to the intensities produced by the sensitometer using a de Vaucouleurs (1968) characteristic curve. The resulting rms deviation was 0.05 mag. The signal-to-noise ratio at the sky brightness level, computed from the formula given by Furenlid, Schoening & Carder (1977), is 32.

The zero-point of the magnitude scale was determined from Melnick & Quintana's (1984) photoelectric photometry. They observed six cluster galaxies with several apertures and, from their $B$ and $V$ photoelectric magnitudes, we computed photographic $b_J$ magnitudes using the transformation $b_J = B_{pe} - 0.23(B - V)_{pe}$. The rms deviation of the zero-point is 0.10 mag, consistent with the expected errors of photographic photometry.

The digitized image was then analysed with a software package developed at IAG and INPE which produces a list of objects classified as stars or galaxies and a list of parameters such as various kinds of magnitudes, sizes and ellipticities. First, the sky level of the image was represented by a two-dimensional polynomial fitted iteratively with a procedure analogous to that described by Barbon, Benacchio & Capaccioli (1976). Connected pixels with intensities above a chosen threshold over the sky level were associated with objects (stars, galaxies, overlapping images, spurious objects) and for each of these a list of parameters calculated from the moments of its pixel intensities was produced. The classification of each object as a star or 'galaxy candidate' was determined from its position in diagrams of size or mean intensity versus magnitude, where the sequence occupied by single non-saturated stars is well defined (at a given magnitude, galaxy images are larger and have lower mean intensity than stars). The 'galaxy candidates' list contained, besides galaxies, a large number of overlapping objects. All the objects brighter than $b_J \sim 19$ were then checked by eye and the overlapping objects containing galaxies were deblended automatically. The deblending algorithm worked well except for a few galaxies which have been deblended 'by eye'. These objects might have magnitude errors larger than the mean and are marked in the catalogue described below. Finally, all the galaxy images were reprocessed, this time with the sky level computed locally, and all the pixels with surface brightness larger than 25 mag arcsec$^{-2}$ asociated with them were added to give the $b_{25}$ isophotal magnitude of the galaxy.

Equatorial coordinates (1950.0) for the galaxies were determined from PDS measurements of 14 SAO stars in the plate (seven of them inside the digitized region). The formal estimated accuracy of a galaxy position is about ± 1.5 arcsec.

### 2.2 The spectroscopic observations

The spectroscopic observations were made at the Cerro Tololo Inter-American Observatory 4-m telescope during $1\frac{1}{4}$

**Table 1.** Observed fields.

| Field | $\alpha_{1950}$ | $\delta_{1950}$ | $t_{exp}$ (sec) | $N_{gal}$ |
|---|---|---|---|---|
| 1 | 20 09 00.56 | -56 56 09.2 | 2700 | 23 |
| 2 | 20 10 57.19 | -57 19 18.2 | 3600 | 21 |
| 3 | 20 06 41.56 | -57 04 43.3 | 3600 | 21 |
| 4 | 20 07 37.14 | -56 37 51.9 | 3600 | 20 |
| 5 | 20 05 34.24 | -56 36 40.5 | 3600 | 21 |

dark nights on 1990 May 18–19, using the Argus fibre-fed multiple-object spectrograph installed at its prime focus.

The Argus spectrograph consists of a set of 24 independent computer controlled arms, each carrying two adjacent optical fibres of 100 μm diameter (=1.8 arcsec) which are directed to selected configurations of 24 targets and their adjacent sky, within a field of 50 arcmin diameter. These 48 fibres are then routed to a bench-mounted spectrograph located in a thermally and mechanically isolated room outside the telescope room. A diffusing plate at the bench-mounted spectrograph provides a uniformly dispersed 2D illumination field for flat-field calibration of the CCD detector.

A set of five fibre configurations was prepared for these observations, covering the main body of the cluster. Galaxies were selected with priority given to the completion of a sample with measured radial velocities complete to $b_{25}=17.5$. Each field had about two or three galaxies in common with its adjacent fields, providing a check for internal consistency of measurements. Table 1 gives the 1950.0 coordinates of the centres of these fields as well as the total integration time, $t_{exp}$, and number of useful galaxy spectra obtained, $N_{gal}$, for each of them.

The spectra were obtained using a 316 line $mm^{-1}$ grating giving a useful range of 3973 to 5646 Å with a resolution of 6 Å (2 pixels) on a GEC CCD detector. Each field exposure was alternated with a 20-s exposure on a He–Ar arc lamp for wavelength calibrations. High-quality template spectra for cross-correlations measurements were obtained by observing several stellar radial velocity standards of suitable spectral types. A set of five bright Virgo galaxies with good measured radial velocities given by Binggeli, Sandage & Tammann (1985) was also observed, since best cross-correlation results may be obtained when templates constructed from real galaxy spectra are used. All the auxiliary calibration frames for reductions, e.g. bias frame and flat-field frames from the lighted dome, the diffusing plate and the twilight sky, were taken some 2 h before starting the observations. A set of bias frames was also taken at the end of the night.

The standard IRAF 2D spectroscopy package was used for the extraction and wavelength calibration of the observed spectra. Frames were bias-subtracted and divided by the flat-field calibration frame obtained by taking the average of the diffusing plate frames and then correcting it for spectral signatures and variations of the spectrograph transmission with wavelength. We verified that, during the whole night, the position of aperture centroids changed by no more than 0.5 pixel, thus enabling the automatic extraction of the totality of the spectra using the aperture traces and profiles obtained from a single interactive extraction of the spectrum of a high signal-to-noise ratio image obtained by averaging the lighted dome frames. Spectra were then corrected for the fibre-to-fibre transmission using correction factors calculated from the twilight sky spectra. Wavelength calibrations were performed for each fibre using the He–Ar reference lamp exposures. The lines were fitted with a fifth-order polynomial which gave rms errors better than 0.3 pixel (0.9 Å). Dispersion corrections appropriate for each field exposure were then assigned fibre by fibre. Finally, for each field, a median-filtered combined sky spectrum was calculated and subtracted from each object spectrum. Most of the radial velocities were determined using the cross-correlation method of Tonry & Davis (1979). Whenever the spectrum was particularly noisy, the redshift was obtained from H$\beta$ and H$\gamma$ lines, the *G* and Mg I bands (the latter when present) and the *H* and *K* lines. We then used the iterative procedure of Cristiani et al. (1987) to identify other lines in the spectrum and to derive a new average redshift. All the radial velocity calculations have been done using the EvE image processing software developed at the Meudon Observatory.

The spectra were rebinned with a scale of 1 Å $bin^{-1}$, apodized with a cosine bell function and then filtered with a top-hat linear bandpass filter to remove high-frequency noise components. Both absorption- and emission-line positions and cross-correlation procedures were used to derive the velocity, the variation between the different results providing a check on the formal standard deviation computed by the cross-correlation procedure. For those galaxies with both absorption and emission velocities, the mean was calculated after weighting each velocity by the inverse of the squared standard deviation. Template spectra were checked by cross-correlating them with radial velocity standards from the list of Maurice et al. (1984). After some trials we found that the best results were obtained when using as templates the spectrum of the Virgo galaxy NGC 4486B and that of the neighbouring star of NGC 4486A which was accidentally observed. The published radial velocities of NGC 4486B are 1486 and 1540 km $s^{-1}$. We then obtained heliocentric velocities of $1548\pm47$ km $s^{-1}$ for the galaxy and $39\pm14$ km $s^{-1}$ for the star.

In order to estimate the internal accuracy of the radial velocities derived from the cross-correlation procedure, we have fitted a Gaussian profile to the correlation peak displayed; the accuracy of the redshift determination is obtained from the FWHM of the peak. For galaxies having particularly noisy spectra the error measurement is based on the determinations of the measured features, depending on the noise of the spectrum. This source of error is reflected for each galaxy by the dispersion of redshifts from individual lines. (Table 3, below, lists individual heliocentric velocities as well as error estimates.)

Since we have 15 galaxies observed more than once (and two of them were observed three times), we can use the absolute value of the difference between independent measurements of the same galaxy, $|v_1-v_2|$, to estimate the typical global error affecting our observations, due to the several steps in the reduction procedure. If these velocity pairs are drawn from a Gaussian distribution with dispersion $\sigma$, the expected value and standard deviation of $|v_1-v_2|$ are given by

$$\langle|v_1-v_2|\rangle=2\pi^{-1/2}\sigma\pm(2-4/\pi)^{1/2}\sigma/N_{\rm pair}^{1/2}$$
$$=1.128\sigma\pm0.853\sigma/N_{\rm pair}^{1/2}.$$

**Table 2.** Comparison of velocities.

| $N$ (1) | $N_P$ (2) | $V_{our} - V_{Proust}$ km s$^{-1}$ |
|---|---|---|
| 135 | 272 | -5 |
| 176 | 99 | -275 |
| 177 | 191 | -93 |
| 191 | 270 | 2906 |
| 197 | 346 | 2028 |
| 224 | 187 | 6 |

Notes. (1) galaxy number in Table 3 below; (2) galaxy number in Proust et al. (1988).

For our sample with more than one observation per galaxy ($N_{pair}=19$), we have $|v_1-v_2|=112\pm20$ km s$^{-1}$, which corresponds to $\sigma\simeq100$ km s$^{-1}$. This value is in excellent agreement with the dispersion of radial velocities obtained for all galaxies using different templates (98 km s$^{-1}$).

Six of the galaxies were also observed by Proust et al. (1988). In Table 2 we compare the velocity differences between these two sets of observations. Two galaxies in Table 2 (numbers 191 and 197) show a very large discrepancy. From the log sheets of observations made using OPTOPUS we verify that these two galaxies were the only ones observed under very poor weather conditions and were probably misidentified. Excluding these two galaxies, we find our velocities are on average shifted by $-93$ km s$^{-1}$ relative to the Proust et al. (1988) observations, with a standard deviation in the differences of 130 km s$^{-1}$.

Our observations have resulted in 86 new radial velocities for SC2008−57. With 42 radial velocities from the literature (Melnick & Quintana 1981; Proust et al. 1988), a total of 128 radial velocities have now been measured in this cluster, attaining a velocity completeness of 91 per cent for galaxies brighter than $b_{25}=17.5$.

### 2.3 The galaxy catalogue

Table 3 lists the results of our observations as follows: column 1 gives the galaxy number; columns 2 and 3 give the 1950.0 equatorial coordinates; columns 4 and 5 show the Cartesian coordinates (in arcsec) measured over the plate; column 6 lists the $b_{25}$ magnitude; columns 7 and 8 give the heliocentric radial velocities and their errors; columns 9 and 10 give the code for the reference of the radial velocity and any notes on the velocity determination or on the galaxy identification. The catalogue has 203 galaxies and, except for five galaxies with measured velocities, we have included only galaxies brighter than $b_{25}=18.0$, since it is essentially complete up to this magnitude. Two bright galaxies (I4950 and NGC 6862) are obviously foreground objects and, although inside the digitized region, were excluded from the catalogue because their images were saturated. As discussed previously, some galaxies that overlapped strongly with other objects might have magnitude errors larger than the mean. These galaxies are indicated by a colon beside the magnitude in column 6.

**Table 3.** Galaxy catalogue.

| N | $\alpha$ (1950) | $\delta$ (1950) | X arcsec | Y arcsec | $b_{25}$ | $V_{helio}$ km s$^{-1}$ | $\Delta V$ km s$^{-1}$ | Ref. (7) | Notes |
|---|---|---|---|---|---|---|---|---|---|
| 001 | 20 03 56.5 | -56 24 42 | 4747 | 4515 | 17.23 | 16025 | 200 | 3 | |
| 002 | 20 03 55.9 | -56 35 35 | 4741 | 3862 | 17.45 | 14334 | 95 | 1 | (1) |
| 003 | 20 04 08.8 | -56 39 03 | 4631 | 3656 | 17.16 | | | | |
| 004 | 20 04 10.5 | -56 34 58 | 4621 | 3901 | 16.98 | 15104 | 73 | 1 | |
| 005 | 20 04 13.9 | -57 09 56 | 4560 | 1804 | 18.19 | 18558 | 120 | 1 | |
| 006 | 20 04 24.6 | -56 48 08 | 4493 | 3113 | 17.17 | 15456 | 66 | 1 | |
| 007 | 20 04 27.2 | -56 48 57 | 4471 | 3064 | 17.48 | | | | |
| 008 | 20 04 27.9 | -56 51 55 | 4462 | 2886 | 17.23 | 15065 | | 1 | |
| 009 | 20 04 29.5 | -56 48 00 | 4453 | 3121 | 17.69 | | | | |
| 010 | 20 04 38.8 | -56 48 45 | 4376 | 3077 | 17.64 | | | | |
| 011 | 20 04 37.1 | -57 05 09 | 4376 | 2093 | 16.87 | 15960 | 55 | 1 | |
| 012 | 20 04 46.6 | -56 24 01 | 4332 | 4562 | 16.15 | 18327 | 91 | 1 | |
| 013 | 20 05 05.1 | -57 02 44 | 4149 | 2241 | 17.97 | | | | |
| 014 | 20 05 12.4 | -56 39 44 | 4106 | 3622 | 17.44 | 17171 | 74 | 1 | |
| 015 | 20 05 16.6 | -56 42 47 | 4069 | 3439 | 17.98: | | | | |
| 016 | 20 05 20.0 | -56 26 54 | 4052 | 4393 | 17.44 | 16810 | | 1 | |
| 017 | 20 05 21.0 | -56 35 21 | 4038 | 3886 | 17.43: | 15090 | 90 | 1 | |
| 018 | 20 05 34.2 | -56 36 40 | 3928 | 3808 | 17.44 | 17910 | 64 | 1 | |
| 019 | 20 05 35.4 | -56 55 23 | 3907 | 2685 | 17.55 | | | | |
| 020 | 20 05 46.9 | -56 30 26 | 3827 | 4183 | 17.61 | | | | |
| 021 | 20 05 48.4 | -56 49 33 | 3804 | 3036 | 17.90 | | | | |
| 022 | 20 05 50.5 | -56 51 10 | 3785 | 2939 | 17.14 | 18230 | 65 | 1 | |
| 023 | 20 06 00.0 | -56 36 47 | 3715 | 3803 | 17.88 | | | | |
| 024 | 20 05 59.2 | -57 05 06 | 3707 | 2104 | 17.61 | 18573 | 100 | 1 | |
| 025 | 20 06 02.7 | -56 28 02 | 3698 | 4328 | 16.46 | 15053 | 72 | 1 | |
| 026 | 20 06 02.8 | -56 50 41 | 3685 | 2969 | 17.53 | | | | |
| 027 | 20 06 07.9 | -56 48 30 | 3644 | 3101 | 17.32 | 16458 | 66 | 1 | |
| 028 | 20 06 10.7 | -56 40 26 | 3625 | 3585 | 17.78: | 18146 | 62 | 1 | |
| 029 | 20 06 10.8 | -56 44 52 | 3622 | 3319 | 17.61 | | | | |
| 030 | 20 06 18.0 | -56 22 36 | 3574 | 4655 | 17.75 | | | | |
| 031 | 20 06 19.7 | -56 39 00 | 3552 | 3671 | 17.09 | 17609 | 89 | 1 | |
| 032 | 20 06 19.2 | -56 53 38 | 3549 | 2793 | 17.17: | 16921 | 66 | 1 | |
| 033 | 20 06 22.1 | -56 21 00 | 3540 | 4752 | 16.31 | 15778 | 81 | 1 | (2) |
| 034 | 20 06 22.0 | -56 36 49 | 3534 | 3803 | 16.95: | | | | |
| 035 | 20 06 27.6 | -56 27 19 | 3492 | 4373 | 17.78 | | | | |
| 036 | 20 06 24.7 | -57 14 22 | 3495 | 1550 | 18.65 | 15940 | 84 | 1 | |
| 037 | 20 06 28.6 | -56 26 38 | 3484 | 4414 | 16.77 | 15656 | 58 | 1 | |
| 038 | 20 06 31.7 | -56 31 00 | 3456 | 4152 | 17.92 | | | | |
| 039 | 20 06 30.0 | -57 10 55 | 3453 | 1757 | 18.66 | 16662 | 100 | 1 | |
| 040 | 20 06 33.4 | -56 30 39 | 3442 | 4173 | 17.12 | 15330 | | 2 | |
| 041 | 20 06 38.6 | -57 11 34 | 3383 | 1719 | 17.11 | 15812 | 47 | 1 | |
| 042 | 20 06 43.9 | -56 30 46 | 3355 | 4167 | 17.03 | 17415 | | 2 | |
| 043 | 20 06 45.4 | -56 41 21 | 3339 | 3532 | 17.97 | | | | |
| 044 | 20 06 47.0 | -56 40 49 | 3326 | 3564 | 16.08 | 14030 | 240 | 3 | |
| 045 | 20 06 47.2 | -56 49 54 | 3321 | 3019 | 17.71 | | | | |
| 046 | 20 06 45.0 | -57 28 47 | 3324 | 686 | 17.59 | | | | |
| 047 | 20 06 49.0 | -56 50 44 | 3306 | 2969 | 17.79 | | | | |
| 048 | 20 06 47.6 | -57 27 18 | 3304 | 775 | 17.55 | | | | |
| 049 | 20 06 50.8 | -56 41 52 | 3294 | 3501 | 17.27 | 15907 | 89 | 1 | |
| 050 | 20 06 50.4 | -56 49 17 | 3295 | 3056 | 15.12: | 16890 | 70 | 3 | |
| 051 | 20 06 51.3 | -56 49 54 | 3287 | 3019 | 16.67: | 17156 | 64 | 1 | |
| 052 | 20 06 52.5 | -56 59 15 | 3274 | 2458 | 17.60 | 19185 | 76 | 1 | (3) |
| 053 | 20 06 53.0 | -56 49 35 | 3273 | 3038 | 17.55: | | | | |
| 054 | 20 06 54.0 | -56 34 52 | 3270 | 3921 | 16.28 | 15540 | 85 | 2 | |
| 055 | 20 06 54.9 | -56 38 47 | 3261 | 3686 | 17.77 | 16821 | 67 | 1 | |
| 056 | 20 06 55.6 | -56 32 20 | 3258 | 4073 | 16.47 | 15060 | 120 | 2 | |
| 057 | 20 06 57.7 | -56 47 31 | 3236 | 3162 | 17.07 | 17605 | 56 | 1 | |
| 058 | 20 06 58.9 | -56 48 47 | 3225 | 3087 | 17.20 | 18320 | 50 | 3 | |
| 059 | 20 06 59.7 | -56 51 47 | 3218 | 2907 | 16.98 | 14408 | 97 | 1 | (4) |
| 060 | 20 06 60.0 | -56 54 49 | 3214 | 2725 | 16.01: | 17868 | 60 | 1 | |
| 061 | 20 06 59.4 | -57 26 09 | 3209 | 845 | 17.49 | | | | |
| 062 | 20 07 05.2 | -56 40 41 | 3176 | 3573 | 17.68: | | | | |
| 063 | 20 07 07.8 | -56 32 15 | 3157 | 4079 | 16.88 | 17650 | | 2 | |
| 064 | 20 07 06.9 | -57 09 14 | 3154 | 1860 | 17.14 | 15918 | 77 | 1 | |
| 065 | 20 07 08.6 | -56 50 51 | 3145 | 2963 | 16.25 | 16125 | 60 | 1 | |
| 066 | 20 07 12.9 | -57 06 19 | 3106 | 2035 | 17.76 | 18940 | 75 | 2 | |
| 067 | 20 07 16.2 | -57 05 14 | 3079 | 2100 | 16.92 | 18049 | 70 | 1 | |
| 068 | 20 07 20.9 | -56 50 58 | 3044 | 2956 | 16.58 | 16430 | 100 | 2 | |
| 069 | 20 07 23.8 | -56 48 04 | 3021 | 3131 | 17.86: | | | | |
| 070 | 20 07 24.8 | -56 49 59 | 3012 | 3016 | 17.52 | 15960 | 50 | 3 | |
| 071 | 20 07 25.9 | -56 42 44 | 3005 | 3451 | 17.20 | 17301 | 73 | 1 | |
| 072 | 20 07 27.3 | -56 53 02 | 2991 | 2833 | 16.43: | 15760 | 100 | 3 | |
| 073 | 20 07 28.3 | -56 54 12 | 2983 | 2763 | 17.61 | | | | |
| 074 | 20 07 34.6 | -56 53 34 | 2931 | 2801 | 17.59 | 20840 | 120 | 2 | |
| 075 | 20 07 35.5 | -56 59 27 | 2923 | 2448 | 18.00 | | | | |
| 076 | 20 07 35.3 | -57 04 25 | 2923 | 2150 | 16.65: | 18458 | 91 | 1 | |
| 077 | 20 07 37.1 | -56 37 51 | 2914 | 3744 | 17.20 | 16851 | 66 | 1 | |
| 078 | 20 07 37.9 | -56 29 25 | 2909 | 4250 | 17.07: | 16749 | 120 | 1 | |
| 079 | 20 07 36.7 | -57 11 55 | 2911 | 1700 | 17.20 | 16394? | | 1 | |
| 080 | 20 07 39.2 | -56 29 34 | 2898 | 4241 | 17.20 | 16794 | 74 | 1 | |
| 081 | 20 07 41.6 | -57 12 26 | 2871 | 1669 | 17.44 | 16368 | 100 | 1 | |
| 082 | 20 07 48.6 | -57 23 47 | 2812 | 988 | 17.52 | 16300 | 200 | 2 | |
| 083 | 20 07 49.5 | -57 09 25 | 2807 | 1850 | 17.79 | | | | |
| 084 | 20 07 54.3 | -57 04 48 | 2768 | 2127 | 16.82: | 14573 | 69 | 1 | |
| 085 | 20 07 56.1 | -56 53 31 | 2755 | 2804 | 17.43 | 17176 | 53 | 1 | |
| 086 | 20 07 57.0 | -57 14 11 | 2745 | 1564 | 16.38 | 16365 | 42 | 1 | (5) |
| 087 | 20 07 59.5 | -56 39 44 | 2729 | 3631 | 16.92 | 15117 | 63 | 1 | |
| 088 | 20 07 59.2 | -56 54 36 | 2730 | 2739 | 16.17 | 18965 | 70 | 3 | |
| 089 | 20 07 59.8 | -57 10 19 | 2723 | 1796 | 16.92 | 18050 | 75 | 2 | |
| 090 | 20 08 01.1 | -56 57 11 | 2714 | 2584 | 17.63 | | | | |
| 091 | 20 08 02.0 | -56 42 34 | 2708 | 3461 | 17.94 | | | | |

**Table 3** – *continued*

| N | α (1950) | δ (1950) | X arcsec | Y arcsec | $b_{25}$ | $V_{helio}$ km s$^{-1}$ | ΔV km s$^{-1}$ | Ref. (7) | Notes |
|---|---|---|---|---|---|---|---|---|---|
| 092 | 20 08 03.9 | -56 22 42 | 2694 | 4653 | 16.19 | | | | |
| 093 | 20 08 04.6 | -56 48 35 | 2686 | 3100 | 17.86 | | | | |
| 094 | 20 08 05.4 | -56 22 18 | 2681 | 4677 | 16.75 | 15210 | 71 | 1 | |
| 095 | 20 08 07.6 | -56 40 37 | 2662 | 3578 | 15.74 | 15030 | 100 | 2 | |
| 096 | 20 08 11.3 | -56 59 59 | 2630 | 2416 | 17.80 | | | | |
| 097 | 20 08 11.9 | -56 57 40 | 2625 | 2555 | 17.69 | 18006 | 68 | 1 | |
| 098 | 20 08 13.7 | -57 15 42 | 2610 | 1473 | 16.75 | | | | |
| 099 | 20 08 15.6 | -56 47 16 | 2596 | 3179 | 17.90 | | | | |
| 100 | 20 08 15.1 | -57 13 58 | 2599 | 1577 | 16.97 | 16208 | 71 | 1 | |
| 101 | 20 08 15.1 | -57 18 36 | 2598 | 1299 | 17.92 | | | | |
| 102 | 20 08 15.8 | -57 07 02 | 2593 | 1993 | 17.21 | 17350 | 80 | 2 | |
| 103 | 20 08 18.4 | -56 50 45 | 2572 | 2970 | 16.82 | 12820 | 100 | 2 | |
| 104 | 20 08 21.1 | -56 51 32 | 2550 | 2923 | 17.91 | | | | |
| 105 | 20 08 21.5 | -56 56 55 | 2547 | 2600 | 16.37 | 15790 | 210 | 3 | |
| 106 | 20 08 21.9 | -56 57 10 | 2544 | 2585 | 17.17: | 18040 | 90 | 2 | |
| 107 | 20 08 23.1 | -56 24 27 | 2534 | 4549 | 17.97 | 15395 | 57 | 1 | |
| 108 | 20 08 22.7 | -56 59 24 | 2537 | 2451 | 16.47: | 7010 | 50 | 3 | |
| 109 | 20 08 23.2 | -56 59 18 | 2533 | 2457 | 17.80: | 16820 | 120 | 3 | |
| 110 | 20 08 23.2 | -57 26 51 | 2533 | 804 | 16.51 | | | | |
| 111 | 20 08 25.6 | -56 56 51 | 2513 | 2604 | 17.71 | 17365 | 180 | 3 | |
| 112 | 20 08 27.3 | -56 58 36 | 2500 | 2500 | 14.96: | 16490 | 80 | 3 | I4965 |
| 113 | 20 08 29.5 | -56 56 59 | 2482 | 2597 | 16.63: | 14670 | 180 | 3 | |
| 114 | 20 08 30.1 | -56 59 18 | 2477 | 2458 | 17.94 | | | | |
| 115 | 20 08 30.6 | -56 58 37 | 2473 | 2498 | 17.90 | 16395 | 200 | 3 | |
| 116 | 20 08 30.9 | -56 56 53 | 2470 | 2603 | 16.24: | 14530 | 80 | 3 | |
| 117 | 20 08 30.9 | -57 25 42 | 2470 | 873 | 17.50 | 29938 | 51 | 1 | |
| 118 | 20 08 33.4 | -56 51 49 | 2449 | 2906 | 17.07 | 15664 | 60 | 1 | |
| 119 | 20 08 33.6 | -56 40 37 | 2448 | 3579 | 17.82 | 16252 | 69 | 1 | |
| 120 | 20 08 34.1 | -56 39 49 | 2443 | 3626 | 17.18 | 17416 | 64 | 1 | |
| 121 | 20 08 37.2 | -57 21 05 | 2419 | 1150 | 17.03 | 16620 | 80 | 2 | |
| 122 | 20 08 39.2 | -57 00 36 | 2402 | 2379 | 17.57: | | | | |
| 123 | 20 08 40.5 | -56 44 48 | 2391 | 3327 | 17.99 | | | | |
| 124 | 20 08 40.6 | -56 58 49 | 2391 | 2486 | 17.43 | 17240 | 70 | 1 | |
| 125 | 20 08 40.6 | -57 00 48 | 2391 | 2367 | 17.92 | | | | |
| 126 | 20 08 41.5 | -57 09 57 | 2384 | 1818 | 17.92 | 16463 | 75 | 1 | |
| 127 | 20 08 42.2 | -56 37 59 | 2377 | 3736 | 18.00 | 16740 | 56 | 1 | |
| 128 | 20 08 44.4 | -57 27 13 | 2361 | 782 | 17.07 | 15860 | 100 | 2 | |
| 129 | 20 08 46.5 | -57 00 30 | 2343 | 2385 | 17.33 | 16850 | 85 | 2 | |
| 130 | 20 08 51.6 | -57 29 17 | 2304 | 658 | 17.54 | | | | |
| 131 | 20 08 54.1 | -57 36 36 | 2284 | 219 | 17.59 | | | | |
| 132 | 20 08 54.8 | -57 02 13 | 2275 | 2282 | 17.69 | 17464 | 56 | 1 | |
| 133 | 20 08 58.3 | -57 08 13 | 2247 | 1922 | 16.97 | 16116 | 120 | 1 | |
| 134 | 20 09 01.5 | -57 05 54 | 2221 | 2061 | 16.17: | 16130 | 75 | 2 | |
| 135 | 20 09 02.2 | -57 20 23 | 2217 | 1192 | 17.64 | | | | |
| 136 | 20 09 04.4 | -57 19 45 | 2199 | 1230 | 17.94 | | | | |
| 137 | 20 09 04.7 | -57 09 31 | 2195 | 1844 | 17.53 | 32250 | 80 | 2 | |
| 138 | 20 09 05.1 | -57 03 01 | 2191 | 2234 | 17.70 | | | | |
| 139 | 20 09 05.7 | -57 26 05 | 2189 | 850 | 17.35: | | | | |
| 140 | 20 09 05.5 | -57 01 32 | 2188 | 2323 | 16.74: | 19151 | 57 | 1 | |
| 141 | 20 09 07.9 | -57 00 57 | 2168 | 2358 | 17.94: | | | | |
| 142 | 20 09 08.1 | -56 57 32 | 2166 | 2563 | 16.31 | 17909 | 89 | 1 | |
| 143 | 20 09 16.9 | -57 02 21 | 2095 | 2274 | 16.96 | 16025 | 50 | 3 | |
| 144 | 20 09 23.4 | -56 59 01 | 2041 | 2474 | 17.88 | 15854 | 62 | 1 | |
| 145 | 20 09 26.9 | -57 16 22 | 2016 | 1433 | 17.00 | 15828 | 63 | 1 | |
| 146 | 20 09 26.9 | -56 50 47 | 2011 | 2968 | 17.50 | 17418 | 80 | 1 | |
| 147 | 20 09 28.5 | -56 42 34 | 1996 | 3461 | 17.59 | 26065? | | 1 | |
| 148 | 20 09 30.8 | -57 06 53 | 1982 | 2002 | 17.52 | 15954 | 80 | 1 | |
| 149 | 20 09 31.6 | -57 02 43 | 1975 | 2251 | 17.17 | 13550 | 130 | 3 | |
| 150 | 20 09 36.8 | -57 38 18 | 1941 | 116 | 17.78 | | | | |
| 151 | 20 09 37.7 | -56 59 20 | 1924 | 2454 | 17.69: | | | | |
| 152 | 20 09 43.6 | -57 30 05 | 1885 | 609 | 17.57 | | | | |
| 153 | 20 09 46.2 | -56 46 16 | 1851 | 3238 | 16.74 | 16625 | 65 | 1 | |
| 154 | 20 09 52.2 | -57 23 19 | 1813 | 1015 | 16.92 | 16875 | 55 | 1 | |
| 155 | 20 09 54.2 | -56 41 51 | 1784 | 3503 | 17.16 | 18223 | 70 | 1 | |
| 156 | 20 09 55.9 | -57 00 22 | 1776 | 2392 | 17.54 | | | | |
| 157 | 20 09 58.5 | -57 11 29 | 1758 | 1724 | 15.97 | 16330 | 100 | 2 | |
| 158 | 20 09 58.5 | -57 03 57 | 1756 | 2176 | 17.63 | 16670 | 100 | 2 | |
| 159 | 20 09 59.1 | -57 06 48 | 1752 | 2005 | 16.87 | 13260 | 210 | 3 | |
| 160 | 20 09 59.6 | -57 09 03 | 1748 | 1870 | 17.62 | | | | |
| 161 | 20 10 01.4 | -57 00 45 | 1734 | 1768 | 16.68: | 17245 | 50 | 3 | |
| 162 | 20 10 01.7 | -57 07 16 | 1731 | 1977 | 17.85 | | | | |
| 163 | 20 10 02.4 | -57 14 55 | 1728 | 1518 | 17.26 | 15579 | 64 | 1 | |
| 164 | 20 10 04.4 | -57 14 21 | 1711 | 1552 | 17.67 | | | | |
| 165 | 20 10 05.9 | -57 16 35 | 1700 | 1418 | 17.47 | 15510 | 80 | 2 | |
| 166 | 20 10 05.7 | -57 09 34 | 1699 | 1839 | 17.42 | 15367 | 70 | 1 | |
| 167 | 20 10 07.4 | -57 30 16 | 1693 | 597 | 16.52 | 15841 | 61 | 1 | |
| 168 | 20 10 10.6 | -57 06 56 | 1658 | 1997 | 17.53 | | | | |
| 169 | 20 10 12.5 | -57 28 10 | 1651 | 723 | 17.62 | | | | |
| 170 | 20 10 10.8 | -56 32 10 | 1643 | 4083 | 17.98 | | | | |
| 171 | 20 10 17.1 | -57 17 32 | 1610 | 1360 | 18.35 | 16390 | 80 | 2 | |
| 172 | 20 10 24.1 | -57 05 58 | 1548 | 2054 | 17.50 | 18010 | 61 | 1 | |
| 173 | 20 10 32.5 | -57 37 41 | 1494 | 151 | 17.58 | | | | |
| 174 | 20 10 33.5 | -57 25 33 | 1480 | 879 | 17.46 | 16589 | 59 | 1 | |
| 175 | 20 10 46.0 | -56 54 32 | 1364 | 2739 | 17.72 | | | | |
| 176 | 20 10 51.2 | -57 35 10 | 1342 | 300 | 17.08 | | | | |
| 177 | 20 10 51.7 | -57 32 05 | 1337 | 485 | 17.88 | | | | |
| 178 | 20 10 54.4 | -57 27 49 | 1313 | 741 | 17.33 | 28706 | 85 | 1 | (6) |
| 179 | 20 10 56.4 | -57 33 18 | 1300 | 412 | 17.01 | 16822 | 74 | 1 | |
| 180 | 20 10 57.4 | -56 54 31 | 1270 | 2739 | 16.91 | 16244 | 77 | 1 | |
| 181 | 20 11 00.3 | -56 58 48 | 1249 | 2482 | 17.58 | | | | |
| 182 | 20 11 05.7 | -56 45 37 | 1197 | 3272 | 17.36 | 31834? | | 1 | |

**Table 3** – *continued*

| N | α (1950) | δ (1950) | X arcsec | Y arcsec | $b_{25}$ | $V_{helio}$ km s$^{-1}$ | ΔV km s$^{-1}$ | Ref. (7) | Notes |
|---|---|---|---|---|---|---|---|---|---|
| 183 | 20 11 06.1 | -56 45 50 | 1194 | 3259 | 17.69: | | | | |
| 184 | 20 11 08.5 | -57 12 23 | 1190 | 1666 | 17.31 | 15900 | 69 | 1 | |
| 185 | 20 11 09.3 | -57 19 42 | 1188 | 1227 | 16.67 | | | | |
| 186 | 20 11 08.1 | -56 58 27 | 1185 | 2502 | 16.63: | 17673 | 92 | 1 | |
| 187 | 20 11 14.0 | -57 20 14 | 1150 | 1195 | 16.37 | 17327 | 65 | 1 | |
| 188 | 20 11 18.3 | -57 06 47 | 1107 | 2001 | 17.65 | 15213 | 63 | 1 | |
| 189 | 20 11 31.4 | -57 27 03 | 1014 | 784 | 17.98 | | | | |
| 190 | 20 11 34.7 | -57 27 52 | 988 | 735 | 17.87 | | | | |
| 191 | 20 11 42.7 | -57 25 12 | 921 | 894 | 17.65 | | | | |
| 192 | 20 11 46.6 | -57 32 23 | 895 | 463 | 17.87 | | | | |
| 193 | 20 11 47.0 | -57 29 10 | 889 | 656 | 17.12 | 16900 | 73 | 1 | |
| 194 | 20 11 58.2 | -57 33 08 | 802 | 416 | 17.77 | | | | |
| 195 | 20 12 04.5 | -57 12 53 | 735 | 1631 | 18.00 | 16982 | 68 | 1 | |
| 196 | 20 12 15.9 | -56 31 59 | 608 | 4083 | 17.72 | | | | |
| 197 | 20 12 20.6 | -56 59 04 | 593 | 2458 | 17.64 | | | | |
| 198 | 20 12 24.4 | -57 01 00 | 563 | 2341 | 16.98 | 16159 | 61 | 1 | |
| 199 | 20 12 49.4 | -57 20 59 | 378 | 1139 | 16.23 | 16695 | 61 | 1 | |
| 200 | 20 12 57.5 | -57 28 51 | 321 | 666 | 17.72 | | | | |
| 201 | 20 13 00.6 | -57 24 03 | 291 | 954 | 18.02 | 17207 | 75 | 1 | |
| 202 | 20 13 04.8 | -57 35 42 | 269 | 254 | 17.99 | | | | |
| 203 | 20 13 01.3 | -57 09 16 | 270 | 1841 | 17.39 | 18416 | 100 | 1 | |

Notes. (1) Two galaxies in the line of sight. The first one is at $V = 4476 \pm 94$ km s$^{-1}$. (2) H$\gamma$ and H$\beta$ in emission: 15 950 km s$^{-1}$; second measurement: 15 784 km s$^{-1}$. (3) Foreground galaxy at 9298 km s$^{-1}$? (4) H$\beta$ in emission: 14 338 km s$^{-1}$; second measurement: 14 487 km s$^{-1}$. (5) Also Fairall 339 (see Fairall 1981). Seyfert 1 type galaxy. Measurements made on hydrogen, Fe II and [O III] emission lines. (6) [O II] 3727 line in emission: 28 634 km s$^{-1}$. (7) References of radial velocities: 1 – present work; 2 – Proust et al. (1988); 3 – Melnick & Quintana (1981).

## 3 THE GALAXY DISTRIBUTION

### 3.1 Field density

We have estimated the field density, i.e. the surface density of galaxies in the cluster field that are not cluster members, from our velocity measurements. 99 of the 109 galaxies in Table 3 with $b_{25} \leq 17.5$ have measured velocities and only four probably are not cluster members (see Section 5). Considering the area studied ( ~ 1.8 square degrees), this corresponds to about 2.5 galaxies per square degree brighter than $b_{25} = 17.5$, or 5 galaxies per square degree brighter than $b_{25} = 18.0$ (assuming a uniform Euclidean distribution for the field galaxies). This density is less than half of that computed with Rainey's luminosity function (Abell 1977), used by Abell et al. (1989) for correcting galaxy counts in southern clusters from field contamination. However, since our estimate of the field density is based on only four galaxies, its Poisson error is 50 per cent and the difference between our value and that derived using Rainey's luminosity function is only about $2\sigma$. It is important, however, to stress the problem of using, in single-cluster studies, 'general' field luminosity functions, since the luminosity functions of bright galaxies may differ from samples measured in the northern and southern hemispheres (e.g. Davis & Huchra 1982), and they can fluctuate significantly on small scales due to the superposition of distinct groups or clusters along the line of sight.

### 3.2 Classification and richness

A plot of all the galaxies in our catalogue is shown in Fig. 1. SC2008 − 57 has two dominant galaxies, both classified as D by Melnick & Quintana (1981). The brightest galaxy is I4965. This cluster was classified by Abell et al. (1989) as IR: and as I–II in the Abell (1965) and Bautz & Morgan (1970)

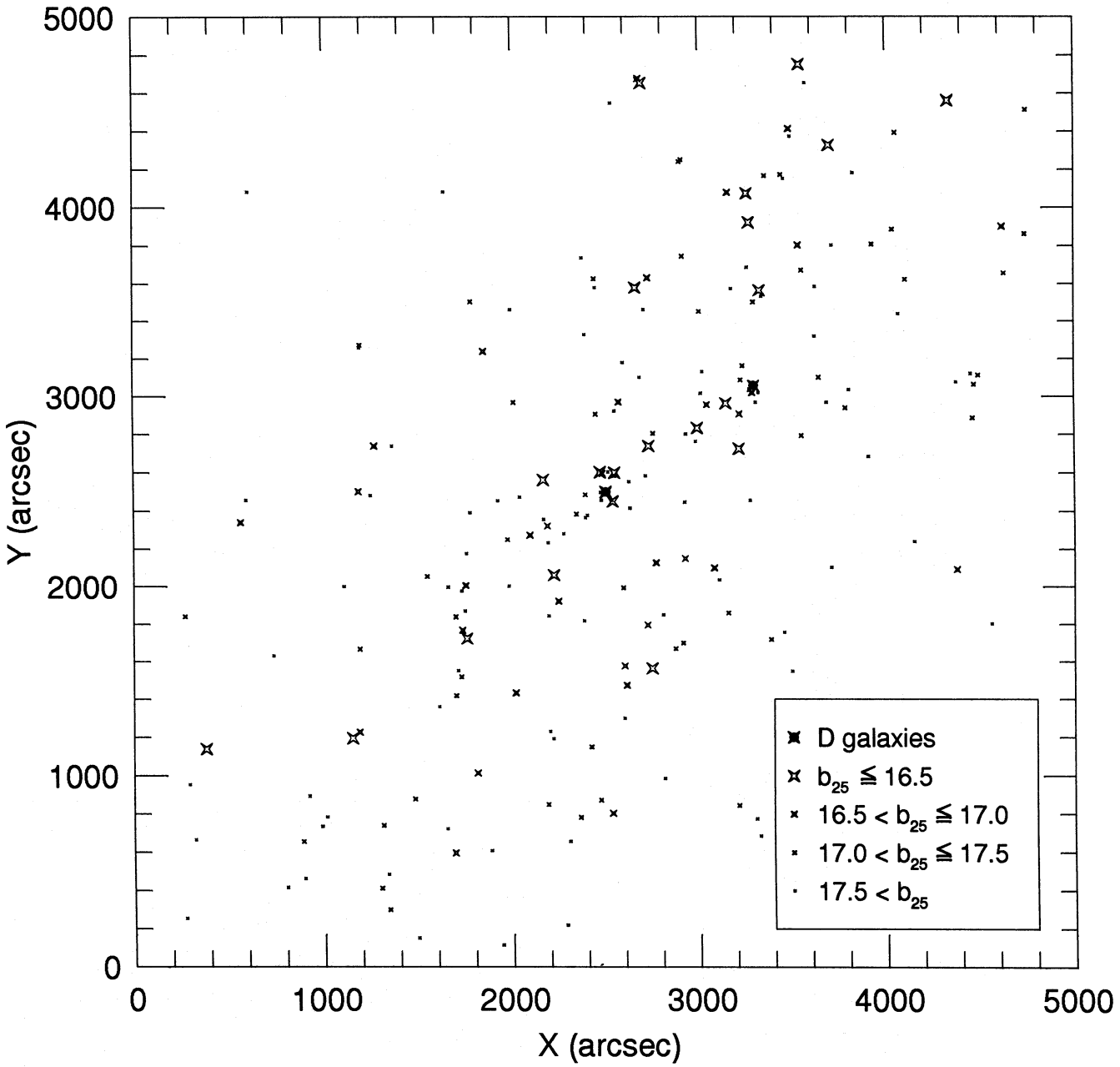


**Figure 1.** Spatial distribution of all the galaxies of the catalogue. Symbol sizes are proportional to galaxy magnitude (see box). The two D galaxies are at (2500, 2500) and (3295, 3056). Axes are in arcsec (north at top, east at left).

systems, respectively. It is better described, however, in the revised Rood and Sastry system (Struble & Rood 1982, 1984), where it is classified as L-type (line) (Bahcall 1977) since its nine brightest galaxies show an obvious collinear arrangement, with fainter galaxies distributed in a bar-like fashion around them. Only 4 per cent of the clusters with distance class $D \leq 4$ in the statistical sample of the Abell (1958) catalogue are of this type. The overall flattening of the galaxy distribution shown in Fig. 1 seems to confirm the classification as L-type, since a classification based only on the positions of the brightest galaxies is problematic, as discussed by Chapman, Geller & Huchra (1987). They have shown, by Monte Carlo simulations, that more than 2 per cent of intrinsically spherical clusters may be erroneously classified as L-type by the positions of the brightest galaxies on the plane of the sky. A least-square fitting on the coordinates of the nine brightest galaxies gives a position angle of 135° for the cluster axis.

The cluster richness depends on the adopted cluster centre (and on the field galaxy surface density). If we assume that the cluster is centred on its brightest galaxy, the number of galaxies with magnitudes in the interval between $m_3$ and $m_3+2$ (where $m_3$ is the magnitude of the third-brightest galaxy) inside one Abell radius ($=1.7/z$ arcmin) is $N_A=105$ (richness class $R=2$), after correcting for the field contamination. Another richness estimate (Bahcall 1977) consists of

counting the number of galaxies with magnitudes less than $m_3+2$ inside a circle of radius 0.25 Mpc, which corresponds roughly to the core radius of a typical cluster. In this case we have $N_B=15$ galaxies. Comparing these values with those obtained for the well-studied Coma cluster [$N_A=106$ (Abell et al. 1989) and $N_B=28$ (Bahcall 1977)], we conclude that SC2008 − 57 is just as rich but less centrally concentrated than Coma.

### 3.3 Structure of the galaxy distribution

An isodensity map of SC2008 − 57 is shown in Fig. 2, where the galaxy density was calculated in a $100\times100$ grid from the distance to the sixth neighbour (Casertano & Hut 1985). We can see two strong galaxy concentrations in this figure. The main concentration is centred on the brightest cluster galaxy, whereas the substructure is centred near the second-brightest galaxy. Substructures have been found in several clusters (Geller & Beers 1982; Dressler & Shectman 1988), often around the brightest galaxies, and their presence is interpreted as evidence of the dynamical youth of a large fraction of the observed clusters. The relative importance of the substructure with respect to the main galaxy concentration can be estimated from the ratio of the number of galaxies brighter than $b_{25}=18$ inside one Bahcall radius around each of the two brightest galaxies, 20:13. In Section 5 we discuss the kinematical evidence for the reality of this substructure.

The overall flattening of the galaxy distribution is obvious in Fig. 2. In order to estimate quantitatively its ellipticity, we have used the method discussed by Carter & Metcalfe (1980) with the centre fixed on the cluster brightest galaxy. In this method the elliptical parameters are derived iteratively from the first five moments of the distribution of the projected positions. The resultant ellipticity $(1-b/a)$ for the galaxies brighter than $b_{25}=18.0$ is fairly large, $0.82\pm0.10$, and the position angle is $134°\pm4°$, coincident with the position angle of the 'line' defined by the nine brightest galaxies.

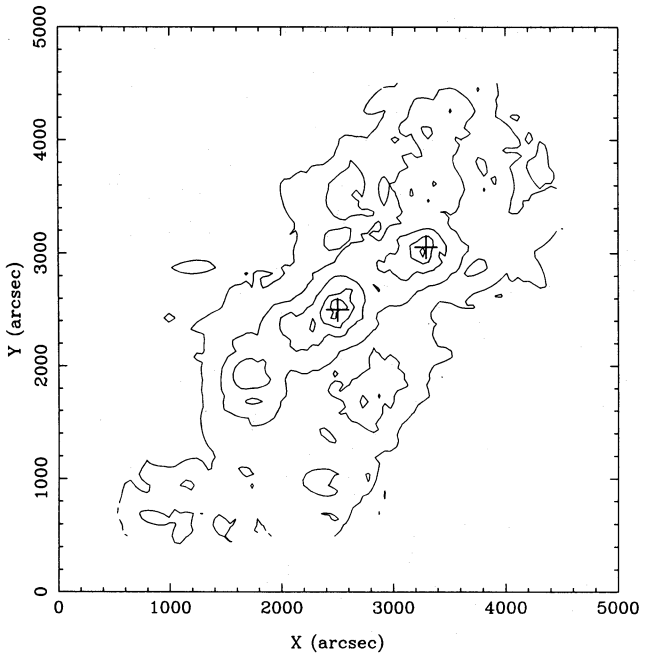


**Figure 2.** Isodensity contour map of galaxies brighter than $b_{25}=18.0$. The minimum level plotted is 100 galaxies per square degree and the separation between consecutive logarithmically spaced levels is 0.35. Contours for which the distance to the sixth neighbour is larger than the distance to one of the borders of the digitized region were not plotted. The positions of the two D galaxies are indicated with crosses.

In Fig. 3 we show the X-ray map of the cluster central region obtained by the *Einstein* satellite (kindly provided for us by C. Jones). It shows extended emission centred on the cluster brightest galaxy, and only a small emission excess is apparent at the position of the second brightest galaxy. The X-ray isophotes have approximately elliptical shapes with the major axis in the same direction as the line joining the two cluster brightest galaxies. Superposed over the extended emission there are three point sources: the south-eastern source is associated with the F5 star SAO 246498, whereas the north-western and south-western sources are associated with galaxies 072 and 086, respectively. The latter source is classified as Seyfert 1 by Fairall (1981).

## 4 LUMINOSITY DISTRIBUTION

### 4.1 Luminosity function

The differential luminosity function of SC2008 − 57 is shown in Fig. 4. Absolute magnitudes were computed from the distance modulus $b_{25}-M_{25}=36.51$, which includes the $K$-term (from Coleman, Wu & Weedman 1980), the correction for interstellar absorption (from Burstein & Heiles 1982) and the correction for the $(1+z)^4$ isophotal dimming [computed with the model of Cameron (1990) for early-type galaxies]. The cluster luminosity function was represented by a Schechter (1976) function and the field luminosity function was assumed to be that of a uniform spatial distribution. The Schechter function has two parameters, $\alpha$ and $L^*$ (or $M^*$), as well as a normalization constant, and is essentially a power law at faint luminosities ($L\ll L^*$) and an exponential for $L\gg L^*$. These parameters were computed by a least-square fitting following the procedure described by Lugger (1986), excluding the two brightest galaxies. The fits were performed with $\alpha$ both varying and fixed at $-1.25$ (Schechter 1976). Allowing $\alpha$ to vary, the best fit to the data (with 0.5-mag bins) is $\alpha=-1.02\pm0.55$, $M^*_{25}=-19.28\pm0.43$. With $\alpha=-1.25$ we have $M^*_{25}=-19.45\pm0.15$. The inclusion of the two brightest galaxies does not change these results significantly. It should be pointed out that the large error in $\alpha$ is mainly due to the fact that our sample is not deep enough to probe the faint end of the luminosity function well. The values for $M^*_{25}$ may be compared with the 'universal' value usually found for this parameter. The mean value obtained in the CfA Redshift Survey is $M^*_{B0}=-19.4$ (Davis & Huchra 1982). Considering that the difference between the $B$ and $b_j$ passbands is about 0.25 for early-type galaxies, our values for $M^*_{25}$ are well in agreement with the 'universal value'. Our value of $\alpha$ is also consistent, within the errors, with Schechter's preferred value of $-1.25$. Its nominal value, however, suggests a somewhat flatter faint end. Several clusters show a similar behaviour, as discussed by Dressler (1978) and Lugger (1986). The value of $\alpha$, however, is expected to be strongly dependent on the cluster morphological content (Binggeli, Sandage & Tammann 1988). We conclude that, taking into account the errors in the para-

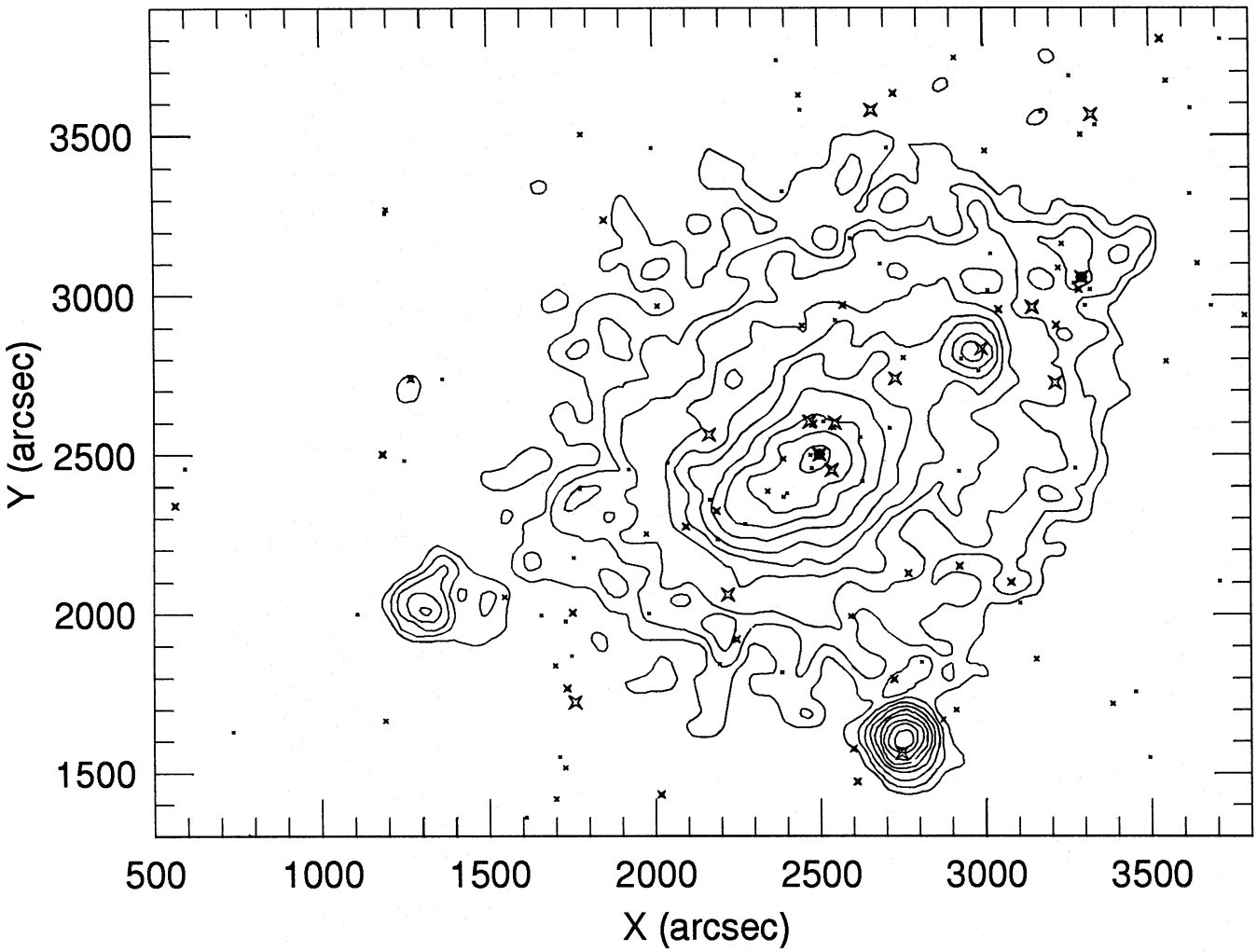


**Figure 3.** X-ray surface brightness contours from the *Einstein* satellite superposed on the galaxy distribution for the central region of the cluster. The faintest X-ray contour is about $3\sigma$ above the background. Symbol sizes as in Fig. 1. The three point sources referred to in the text are at (1300, 2000), (3000, 2800) and (2750, 1600) for the south-eastern, north-western and south-western sources, respectively.

meters describing the Schechter function, the luminosity function of SC2008−57 is similar to that usually found in clusters.

### 4.2 Luminosity segregation

The fact that, in this cluster, the brightest galaxies are aligned along the major axis of the galaxy distribution suggests the presence of luminosity segregation. Luminosity segregation is thought to be a manifestation of mass segregation due to the expected correlation between mass and luminosity among galaxies of same morphological type. After the initial collapse and violent relaxation of the cluster, two-body interactions tend to promote kinetic energy equipartition among cluster galaxies. Chandrasekhar (1942) has shown that a massive galaxy moving among lighter objects has its movement retarded due to dynamical friction. The massive galaxies tend, as a consequence, to fall towards the bottom of the cluster potential well, while the lighter galaxies tend to expand. As a result, a mass segregation is established in the cluster, with massive galaxies showing a more concentrated distribution. The time-scale for mass segregation is, however, poorly known, due to uncertainties in the $M/L$ ratio for cluster galaxies as well as in the total cluster mass distribution, but it might be less than one Hubble time, at least in the densest regions of a cluster.

The evolution due to the dynamical friction of non-spherical clusters was studied analytically by Binney (1977), under the hypothesis that these clusters are sustained by an ellipsoidal velocity distribution. Due to the dynamical friction the more massive galaxies displace towards the symmetry axis (for prolate clusters) or to the symmetry plane (for oblate clusters) and their distribution becomes progressively more aligned (or flatter). Hence dynamical friction could explain the form of type-L clusters if, of course, there is enough time for it to work.

The mean projected density of galaxies within a given magnitude interval can be used to study the luminosity segregation. This estimator is related to the probability of finding a galaxy of a given magnitude in regions of the cluster having local densities within a given range. If the mass segregation is real, massive galaxies should be found preferentially in dense

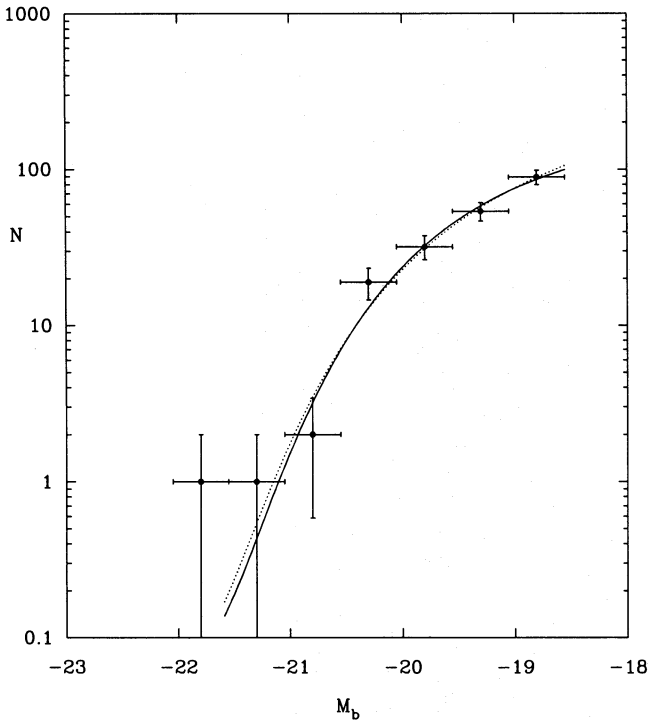


**Figure 4.** Differential luminosity function of SC2008 − 57. The solid line is the best-fitting Schechter function to the data with $\alpha$ free; the dotted line is the best fit to the data with $\alpha = -1.25$. The two cluster brightest galaxies were excluded from the least-square fits.

**Table 4.** Luminosity segregation.

| $b_{25}$ | $\Sigma^{(1)}$ gal. (sq. degree)$^{-1}$ | $N^{(2)}$ | $\Sigma^{(3)}$ gal. (sq. degree)$^{-1}$ | $N^{(4)}$ |
|---|---|---|---|---|
| 14.5-16.5 | 646±99 | 19 | 249±35 | 13 |
| 16.5-17.0 | 342±86 | 28 | 223±28 | 25 |
| 17.0-17.5 | 289±58 | 44 | 173±20 | 39 |
| 17.5-18.0 | 372±41 | 73 | 223±14 | 62 |

Notes. (1) Mean projected galaxy density; 1 $\sigma$ errors computed from the variance of the scrambled samples; (2) number of galaxies in the magnitude bin; (3) mean projected galaxy density and 1 $\sigma$ errors from the variance of the scrambled samples, excluding from the mean those galaxies within 200 arcsec of the two brightest galaxies; (4) number of galaxies in the magnitude bin excluding galaxies within 200 arcsec of the two brightest galaxies.

regions. We have computed the local cluster surface density associated with a galaxy from the distance of its sixth neighbour. Galaxies for which the distance to the sixth neighbour is larger than the distance to any of the borders of the digitized image were excluded from this analysis. We then grouped the galaxies in 0.5-mag bins (except for the brightest bin) and computed the mean density for galaxies within each magnitude bin. The same analysis was done with 1000 scrambled samples, where we redistributed the galaxy magnitudes randomly, while their positions were kept fixed. These scrambled samples allow us to establish the error bars of our mean density estimates for the cluster data, taking into account the statistical fluctuations intrinsic to the data. The results of this analysis are summarized in Table 4 and Fig. 5.

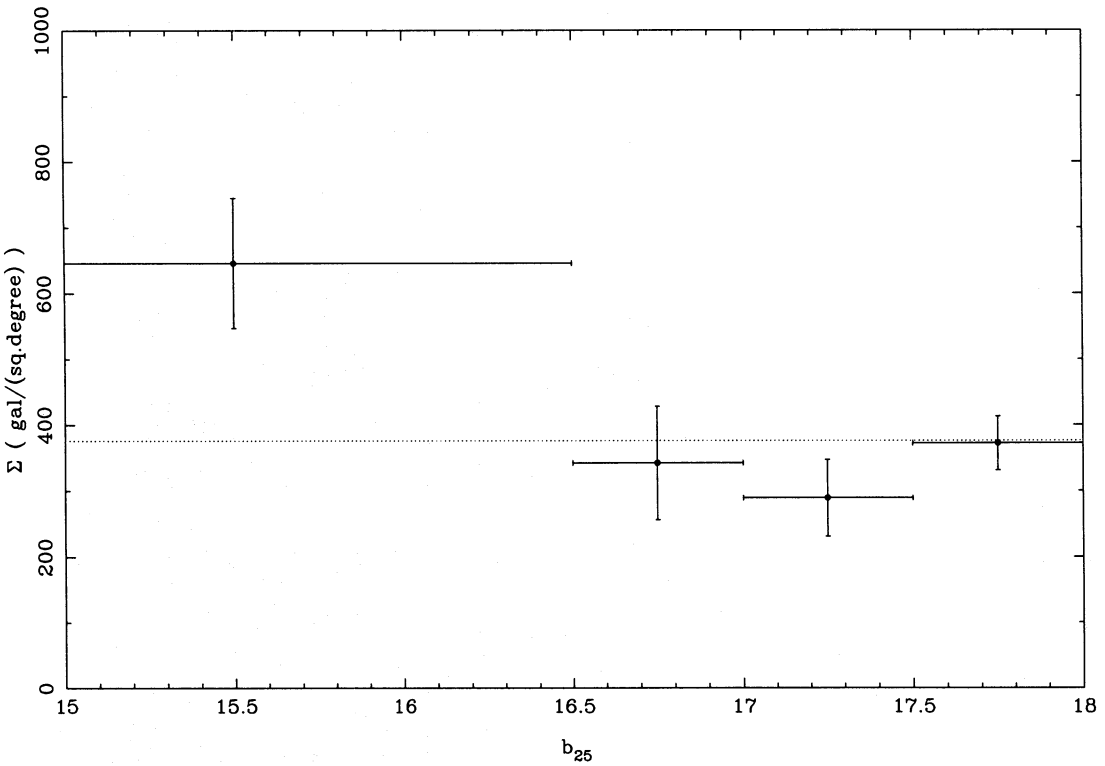


**Figure 5.** Mean galaxy density (galaxies per square degree) as a function of magnitude. The error bars have been computed from the variances of 1000 scrambled samples. The dotted line indicates the cluster mean density.

The galaxies in the brightest bin are indeed found preferentially in dense regions. The mean galaxy density of objects in this bin is about $2.7\sigma$ above the typical galaxy density of the cluster, 376 galaxies per square degree. For magnitudes fainter than 16.5, the differences between the mean galaxy density for a given magnitude interval and the typical galaxy density of the cluster are always smaller than $1.5\sigma$. Actually a large part of this segregation is due to galaxies inside the cluster core, and substructure. In order to demonstrate this point, we have repeated the above calculation, excluding all galaxies within 200 arcsec of the two brightest galaxies. The results of this exercise are also presented in Table 4. Although, even in this case, the brightest galaxies have the largest mean galaxy projected density, this value is now only $1\sigma$ above the overall mean density, 212 galaxies per square degree. Six out of the 19 brightest galaxies are in the two density peaks shown in Fig. 2 and are responsible for most of the observed luminosity segregation.

This result suggests that the observed luminosity segregation is not due to dynamical friction in the cluster as a whole but to friction within the subclusters. As discussed by Merritt (1984), dynamical friction is more effective inside substructures because of the lower velocity dispersions and, besides producing luminosity segregation, it may have helped form the D galaxies themselves, through mergers (in the next section we will present evidence for low velocity dispersion within each subcluster). The flattening of the cluster, in this case, was not produced by dynamical friction; instead two subclusters, one around each D galaxy, are merging. This leads to the overall flattening of the galaxy distribution and to the observed substructure.

## 5 VELOCITY ANALYSIS

In Fig. 6 we show the velocity histogram of the 128 heliocentric radial velocities available for SC2008−57. A cone diagram is shown in Fig. 7. The 122 galaxies with heliocentric velocities in the interval between 12 000 and 21 000 km s$^{-1}$ are probably cluster members. For these galaxies the mean velocity is $\langle V \rangle = 16\,557 \pm 117$ km s$^{-1}$ and the corresponding cluster redshift, corrected for solar motion, is $z = 0.05495 \pm 0.00039$, slightly larger than the value $z = 0.053$ obtained by Melnick & Quintana (1981). The velocity dispersion with the corresponding 68 per cent confidence limits, corrected following the precepts of Danese, de Zotti & di Tullio (1980), is $\sigma_{\rm corr} = 1223^{+87}_{-72}$ km s$^{-1}$, where we have imposed an error of 500 km s$^{-1}$ for the velocities in the catalogue for which the velocity error is unknown. We have also computed mean velocities and velocity dispersions with the iterative prescription of Yahil & Vidal (1977), obtaining $\langle V \rangle = 16\,553 \pm 109$ km s$^{-1}$ and $\sigma_{\rm corr} = 1130^{+81}_{-67}$ km s$^{-1}$. Since our velocity sample is more than 90 per cent complete at $b_{25} = 17.5$, it is worth repeating the calculations using the 95 galaxies brighter than this magnitude that are probably cluster members. In this case we have $\langle V \rangle = 16\,409 \pm 129$ km s$^{-1}$ and $\sigma_{\rm corr} = 1192^{+98}_{-79}$ km s$^{-1}$. These results are self-consistent within the errors. They are summarized in Table 5, where in column 1 we give the sample considered, in column 2 the number of galaxies in the sample and in columns 3 and 4 the mean velocity and the cluster velocity dispersion for that sample.

The radial velocity of the cluster brightest galaxy is $16\,490 \pm 80$ km s$^{-1}$, only 67 km s$^{-1}$ less than the cluster

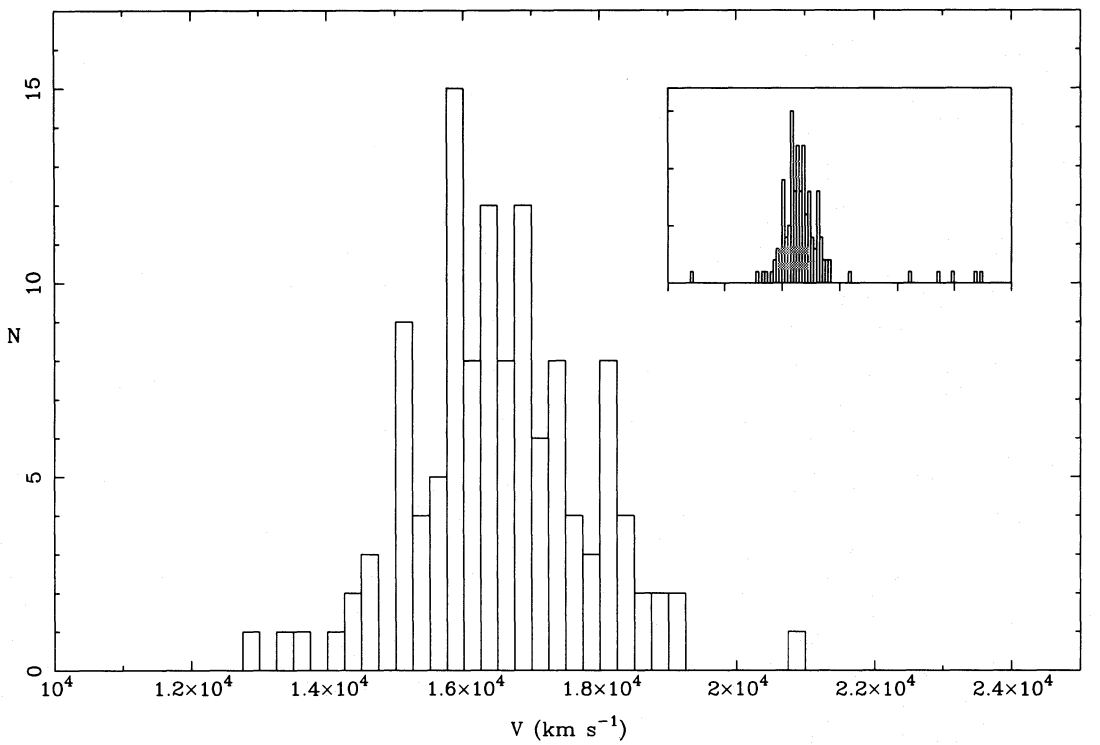


**Figure 6.** Histogram of heliocentric radial velocities for galaxies with velocities between 10 000 and 25 000 km s$^{-1}$. The inset shows the velocity distribution between 5000 and 35 000 km s$^{-1}$, and contains all galaxies with measured velocities in Table 3. Each bin is 250 km s$^{-1}$ wide.

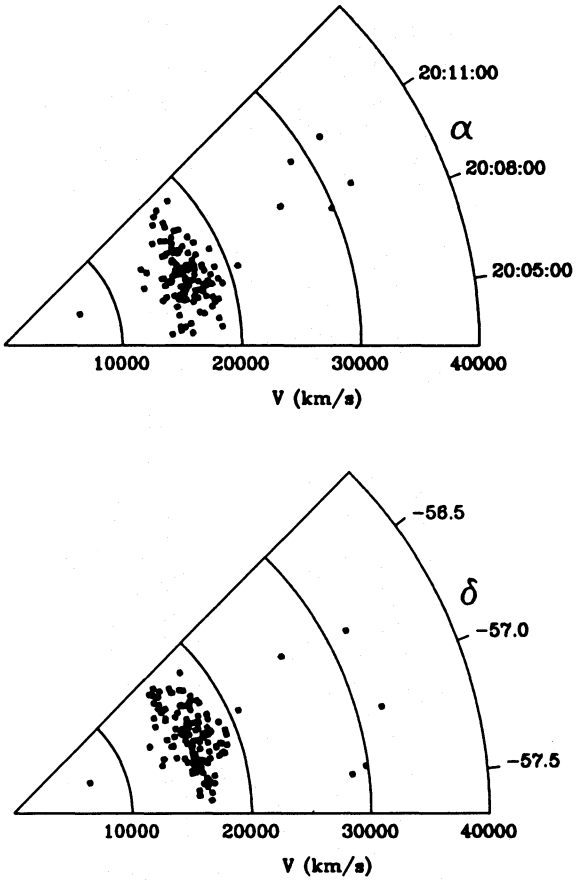


**Figure 7.** Cone diagram of heliocentric velocities for all galaxies with measured velocities in Table 3.

**Table 5.** Mean velocities and velocity dispersions.

| Sample | N | $< V >$ km s$^{-1}$ | $\sigma_{corr}$ km s$^{-1}$ |
|---|---|---|---|
| *all*(1) | 122 | 16557 ± 117 | 1223 |
| *all*(2) | 120 | 16553 ± 109 | 1197 |
| $b_{25} < 17.5$(2) | 95 | 16409 ± 129 | 1262 |

Notes. (a) All galaxies with $12\,000 < V < 21\,000$ km s$^{-1}$; (2) procedure of Yahil & Vidal (1977) applied.

mean velocity (computed from the velocities of the 122 galaxies), suggesting that this galaxy is at the kinematical centre of the cluster (Quintana & Lawrie 1982). The second-brightest galaxy has a radial velocity of $16\,890 \pm 70$ km s$^{-1}$, 400 km s$^{-1}$ larger than the velocity of the brightest galaxy. The value of the cluster velocity dispersion is quite large, but lower than the value previously found by Melnick & Quintana (1981). Only four out of 65 clusters studied by Zabludoff, Huchra & Geller (1990) have $\sigma_{corr}$ larger than 1200 km s$^{-1}$. The X-ray luminosity, however, derived from the *EXOSAT* observations (Piro & Fusco-Femiano 1988) and the above redshift, is $L_X = 2.5 \times 10^{44}$ erg s$^{-1}$, and a value of $\sigma_{corr}$ around 1200 km s$^{-1}$ puts this cluster in excellent agreement with the $L_X$–$\sigma$ relation of Mushotzky (1984). This result might be somewhat fortuitous, however, since the map of the galaxy distribution indicates that there is substructure associated with the second-brightest galaxy which may artificially increase the overall velocity dispersion.

We have looked for some kinematical evidence for the substructure using a procedure similar to the one devised by Quintana & Ramirez (1991). Starting from the position of each of the two brightest galaxies, we computed mean velocities and velocity dispersions as a function of the cumulative number $N$ of galaxies, using the 'pessimistic' criterion of Yahil & Vidal (1977) (see Colless & Hewett 1987). The results are shown in Fig. 8. Fig. 8(b) shows the behaviour of $\sigma_{corr}$ with the cumulative number $N$ of galaxies from the second-brightest galaxy. Despite the large fluctuations, there is a trend for $\sigma_{corr}$ to increase with $N$ from a value of about 800 km s$^{-1}$, significantly lower than the overall cluster value. This result may be interpreted as evidence that the substructure is real. Most of the galaxies in the neighbourhood of the second-brightest galaxy might form a satellite population, as observed in several other clusters (Cowie & Hu 1986; Bothun & Schombert 1988; Quintana & Ramirez 1991). For the galaxies around the cluster brightest galaxy (Fig. 8a), the velocity dispersion is almost equal to the overall cluster dispersion, except for the first data point. Considering the six nearest galaxies, the velocity dispersion computed with five of them is $\sigma_{corr} = 647^{+440}_{-143}$ km s$^{-1}$, again significantly below the overall value, suggesting that the cluster brightest galaxy might also have a satellite population. In both diagrams, $\sigma_{corr}$ first increases with $N$ (due to increasing contamination by galaxies of the substructure in Fig. 8a, or by the main galaxy concentration in Fig. 8b) and then falls to the overall cluster velocity dispersion.

The dynamical mass of the cluster was calculated using the mass estimators for self-gravitating systems of equal-mass galaxies from Heisler, Tremaine & Bahcall (1985): virial mass (VM), projected mass (PM), average mass (AM) and median mass (MM). Heisler et al. have noticed that the relative errors of these mass estimates scale with the number of galaxies in the calculation as $N^{-1/2}$. We estimated the errors after calibrating this relation with the results of cluster simulations reported by Quintana & Ramirez (1991). It should be emphasized, however, that systematic errors can be much larger than these formal errors. One important source of systematic error here is the underlying hypothesis that galaxies trace mass. The other is the assumption of overall virial equilibrium, contradicted by the presence of a substructure within the cluster. Our results are shown in Table 6 for the sample of 122 galaxies with measured velocities between 12 000 and 21 000 km s$^{-1}$ and for the subsample of these galaxies with $b_{25} < 17.5$. The results are similar in both cases, giving a mean mass of $2.60 \times 10^{15}$ $M_\odot$ for this cluster.

**Table 6.** Mass estimates.

| Sample | N | VM $10^{14} M_\odot$ | PM $10^{14} M_\odot$ | AM $10^{14} M_\odot$ | MM $10^{14} M_\odot$ |
|---|---|---|---|---|---|
| *all*(1) | 122 | 27.0±4.3 | 28.7±4.6 | 25.6±4.1 | 22.9±3.6 |
| $b_{25} < 17.5$ | 95 | 26.1±4.7 | 28.6±5.1 | 24.9±4.5 | 24.0±4.3 |

Note. (1) All galaxies with $12\,000 < V < 21\,000$ km s$^{-1}$.

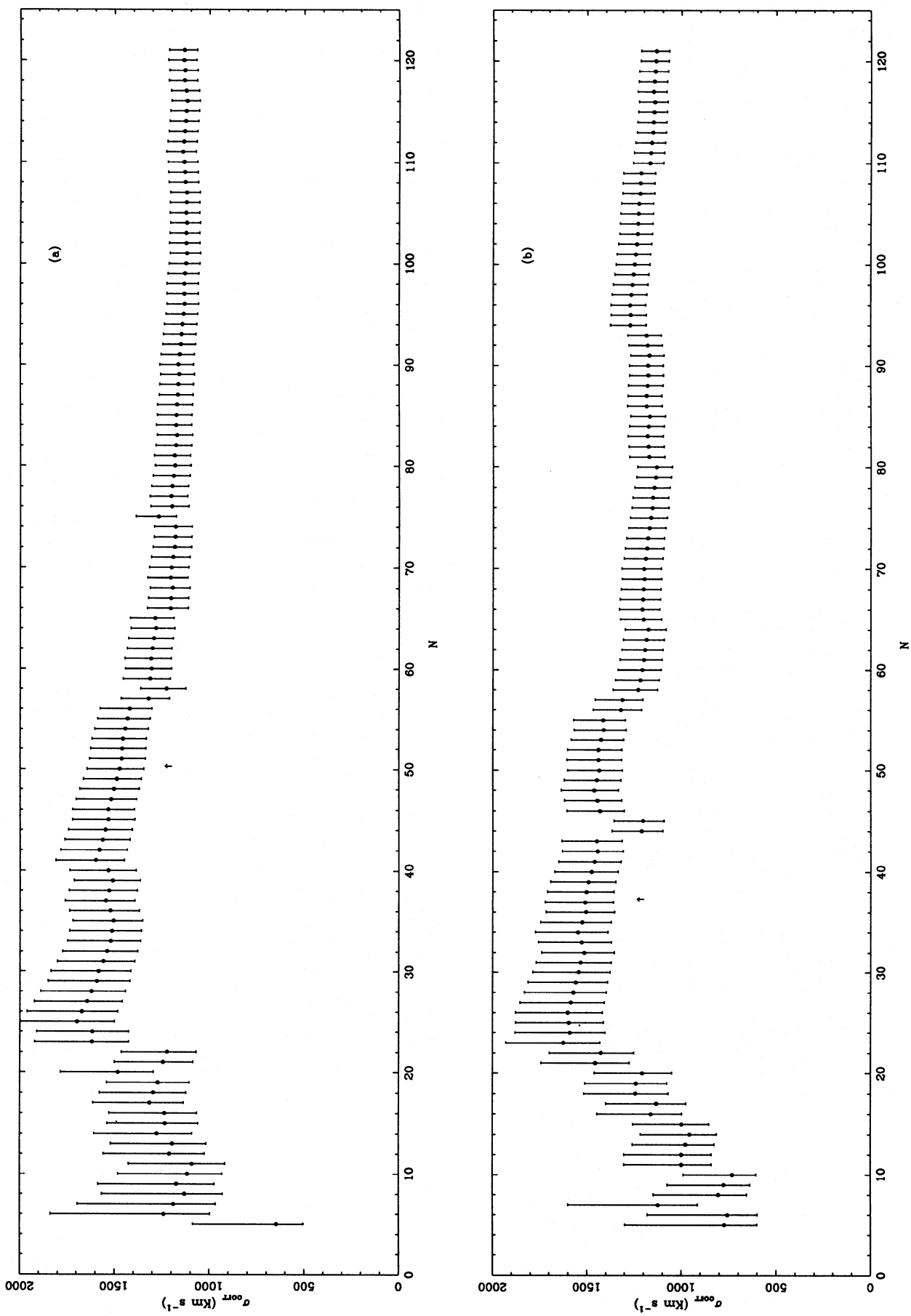


**Figure 8.** Plot of $\sigma_{corr}$ as a cumulative function of the number of galaxies: (a) from the cluster brightest galaxy (the arrow indicates the second-brightest galaxy); (b) from the cluster second-brightest galaxy (the arrow indicates the cluster brightest galaxy).

We have used a test devised by Chapman et al. (1987) to look for evidence of cluster rotation. The apparent coordinates are rotated so that $X$ is the distance along the cluster axis and $Y$ is the distance from the axis. Then the cumulative distribution as a function of $X$ of cluster members whose velocities are greater than the cluster median (16 477 km $s^{-1}$) is compared with the distribution of those members whose velocities are less than the median. We have used the Kolmogorov–Smirnov two-tail test to determine the statistical significance of this difference. If the cluster is rotating around the $Y$-axis, the probability that these two distributions were drawn from the same parent distribution should be low. Using all the 122 cluster galaxies with measured velocities and a position angle for the $X$-axis of 134°, the value of this probability is high, 67 per cent. We can suppose also that the cluster is rotating around the $X$-axis, but the value of the above probability is also high, 52 per cent. The same analysis was repeated for galaxies with $b_{25} < 17.5$. In this case, also, the two distributions are not significantly different for the cluster rotating either around the $X$-axis or around the $Y$-axis. We conclude that SC2008 − 57 shows no evidence for rotation.

## 6 CONCLUSIONS

We have presented in this paper the results of our photometric and spectroscopic observations of the cluster of galaxies SC2008 − 57 (A3667). We have also examined its spatial, luminosity and velocity distributions using a catalogue with 203 galaxies complete up to $b_{25} = 18.0$ and with 128 radial velocities. The main characteristics of this cluster can be summarized as follows.

(1) The cluster SC2008 − 57 can be classified as type L in the Rood–Sastry system, since its brightest galaxies are almost aligned, with a position angle of 134°. The cluster is highly flattened, with an ellipticity of 0.82.

(2) The galaxy distribution shows two strong concentrations. The main concentration, centred on the cluster brightest galaxy (a D galaxy), is coincident with the peak of X-ray emission. The substructure is around the second-brightest galaxy (also a D galaxy). Most of the galaxies in this substructure seem to be bound to the second-brightest galaxy, forming a dynamical subunit inside the cluster. The extreme flattening of the cluster may at least partially be due to the presence of the substructure.

(3) The cluster shows some evidence of luminosity segregation, with its brightest galaxies found preferentially in dense regions. Most of the luminosity segregation, however, is produced by galaxies associated with the two subclumps around the D galaxies. This result suggests that dynamical friction is effective in subclusters with low velocity dispersions and may be associated with the formation of D galaxies (Merritt 1984).

(4) The cluster overall velocity dispersion is quite high, about 1200 km $s^{-1}$, but consistent with the observed X-ray luminosity. This high value, however, is due at least in part to the presence of the substructure.

(5) The cluster mass, derived using several estimators, is about $2.6 \times 10^{15}\ M_{\odot}$ but, due to the presence of the substructure, this value may also be overestimated.

## ACKNOWLEDGMENTS

We are pleased to acknowledge the staff of Cerro Tololo Inter-American Observatory for their help in the initial reduction of Argus data, C. Jones for sending us the X-ray map of SC2008 − 57 and Roberto and Elena Terlevitch for useful discussions. LSJ and HVC acknowledge FAPESP for the financial support for their travel to CTIO. LSJ acknowledges a postdoctoral grant from BID/USP which permitted his visit to the Royal Greenwich Observatory, where this paper was written. This work was partially supported by bilateral protocols between CNPq (Brazil) and CNRS (France).

## REFERENCES

Abell G. O., 1958, ApJS, 3, 211
Abell G. O., 1965, ARA&A, 3, 1
Abell G. O., 1977, ApJ, 213, 327
Abell G. O., Corwin H. G., Olowin R. P., 1989, ApJS, 70, 1
Bahcall N. A., ApJ, 217, L77
Barbon R., Benacchio L., Capaccioli M., 1976, Mem. Soc. Astron. Ital., 47, 263
Bautz L. P., Morgan W. W., 1970, ApJ, 162, L149
Bell-Burnell S. J., Chiappetti L., 1984, A&AS, 56, 415
Binggeli B., Sandage A., Tammann G. A., 1985, AJ, 90, 1681
Binggeli B., Sandage A., Tammann G. A., 1988, ARA&A, 26, 509
Binney J., 1977, MNRAS, 181, 735
Bothun G. D., Schombert J. M., 1988, ApJ, 335, 617
Burstein D., Heiles C., 1982, AJ, 87, 1165
Cameron L. M., 1990, A&A, 233, 16
Carter D., Metcalfe N., 1980, MNRAS, 191, 325
Casertano S., Hut P., 1985, ApJ, 298, 80
Chandrasekhar S., 1942, Principles of Stellar Dynamics. Univ. Chicago Press, Chicago
Chapman G. N. F., Geller M. J., Huchra J., 1987, AJ, 94, 571
Coleman G. D., Wu C. C., Weedman D. W., 1980, ApJS, 43, 393
Colless M., Hewett P., 1987, MNRAS, 224, 453
Cowie L. L., Hu E. M., 1986, ApJ, 305, L39
Cristiani S., de Souza R., D'Odorico S., Lund G., Quintana H., 1987, A&A, 179, 108
Danese L., de Zotti G., di Tullio G., 1980, A&A, 82, 322
Davis M., Huchra J. P., 1982, ApJ, 254, 437
de Vaucouleurs G., 1968, Appl. Optics, 7, 1513
Dressler A., 1978, ApJ, 223, 765
Dressler A., Shectman S. A., 1988, AJ, 95, 284
Fairall A. P., 1981, MNRAS, 196, 417
Furenlid I., Schoening W. E., Carder B. E., 1977, Am. Astron. Soc. Photobull., 16, 4
Geller M. J., Beers T. C., 1982, PASP, 94, 421
Heisler J., Tremaine S., Bahcall J. N., 1985, ApJ, 298, 8
Lugger P., 1986, ApJ, 303, 535
Maurice E., Mayor M., Andersen J., Ardeberg A., Benz W., Lindgren H., Imbert M., Martin N., Nordström B., Prévot L., 1984, A&AS, 57, 275
Melnick J., Quintana H., 1981, AJ, 86, 1567
Melnick J., Quintana H., 1984, AJ, 89, 1288
Merritt D., 1984, ApJ, 276, 26
Mushotzky R. F., 1984, Phys. Scripta, 7, 157
Piro L., Fusco-Femiano R., 1988, A&A, 205, 26
Proust D., Mazure A., Sodré L., Capelato H. V., Lund G., 1988, A&AS, 72, 415
Quintana H., Lawrie D., 1982, AJ, 87, 1
Quintana H., Ramirez A., 1991, AJ, 100, 1990
Rood H. J., Sastry G., 1971, PASP, 83, 313

Schechter P. L., 1976, ApJ, 203, 297
Sodré L., Capelato H. V., Steiner J. E., Mazure A., Proust D., 1990, Rev. Mex. Astron. Astrofis., 21, 52
Struble M. F., Rood H. J., 1982, AJ, 87, 7
Struble M. F., Rood H. J., 1984, AJ, 89, 1487
Tonry J., Davis M., 1979, AJ, 84, 1511
Yahil A., Vidal N. V., 1977, ApJ, 214, 347
Zabludoff A. I., Huchra J. P., Geller M. J., 1990, ApJS, 74, 1